MATHEMATICAL BIOSCIENCES
AND ENGINEERING
Volume **9**, Number **4**, October **2012**

doi:10.3934/mbe.2012.9.937

pp. **937–952**

# DYNAMICS OF STOCHASTIC MUTATION TO IMMUNODOMINANCE

Yu Wu, Xiaopeng Zhao and Mingjun Zhang

Department of Mechanical, Aerospace and Biomedical Engineering
University of Tennessee, Knoxville, TN 37996, USA

(Communicated by Sergei S. Pilyugin)

Abstract. Although a virus contains several epitopes that can be recognized by cytotoxic T lymphocytes (CTL), the immune responses against different epitopes are not uniform. Only a few CTLs (sometimes just one) will be immunodominant. Mutation of epitopes has been recognized as an important mechanism of immunodominance. Previous research has studied the influences of sporadic, discrete mutation events. In this work, we introduce a bounded noise term to account for the intrinsic stochastic nature of mutation. Monte Carlo simulations of the stochastic model show abounding complex phenomena, and patterns observed from the numerical simulations shed lights on long term trends of immunodominance.

1. **Introduction.** A virus contains several epitopes that can be recognized by corresponding cytotoxic T lymphocytes (CTL). The immune responses against different epitopes are not uniform. Only the CTLs directed to a few epitopes, sometimes just one, will be dominant. This hierarchical response phenomenon is known as immunodominance [1, 2, 3]. Immunodominance is an interesting phenomenon and has been actively investigated during the last two decades [4, 5, 6, 7, 8, 9, 10, 11, 12, 13, 14, 15, 16, 17]. Competition and predation of the immune species interactions are believed to be the reason of immunodominance. Mathematical models have been developed to explain the mechanism [18, 1, 19, 2, 20, 21, 3, 22, 23]. These models show very complicated dynamics and rich features. The emergence of new virus variants may give rise to peaks in viral concentrations, the so-called "antigenic drift" [24, 18, 25, 26, 27]. Even in the absence of mutations, fluctuations and oscillations in the concentration of virus variants and immune responses against different epitopes, known as "antigenic oscillation", are observed [1, 19]. As an important consequence of the emergence of escape mutants, shifting of the immunodominance may lead to disease progression [1, 19]. Memory cytotoxic T lymphocyte precursors (CTLp) are important for efficient virus control [20].

Previous research treats mutation as discrete events, which occur at prescribed times with deterministic mutation rates [22]. To account for the intrinsic uncertainties in escape mutation, we introduce a stochastic process to the immunodominance model developed by Nowak *et al.* [1]. The stochastic mutation term has great influences on both the instant state and the long-term trend of the immune response.

2000 *Mathematics Subject Classification.* Primary: 92D25, 65C05; Secondary: 60H10, 62P10.
*Key words and phrases.* Immunodominance, mutation, stochastic dynamics, Monte Carlo simulation.

The model shows many interesting dynamical behaviors, and can be used to explain some experimental results from longitudinal studies.

2. **The stochastic mutation model.** Nowak, May and Sigmund developed an immune model, which considers two mutants in epitope $A$ (labeled as $A_1$ and $A_2$) and a single variant in epitope $B$ [1]. Here, we modify the model of Nowak et al. as follows:

$$\begin{aligned}
\dot{V}_1' &= V_1' \left(r_1' - p_1' X_1' - q' Y'\right) - \frac{1}{2}\varepsilon r_1' V_1' \left(1 + \xi'(t')\right) \\
\dot{V}_2' &= V_2' (r_2' - p_2' X_2' - q' Y') + \frac{1}{2}\varepsilon r_1' V_1' \left(1 + \xi'(t')\right) \\
\dot{X}_1' &= X_1' (c_1' V_1' - b') \\
\dot{X}_2' &= X_2' (c_2' V_2' - b') \\
\dot{Y}' &= Y' \left[k' (V_1' + V_2') - b'\right]
\end{aligned} \tag{1}$$

where $V_1'$ and $V_2'$ denote the concentration of two virus variants. Note that virus 1 contains epitopes $A_1$ and $B$, and virus 2 contains epitopes $A_2$ and $B$. The variables $X_1'$, $X_2'$, and $Y'$ denote the CTL clones directed at epitope $A_1$, $A_2$, and $B$, respectively. Replication rates of the viruses are denoted by $r_1' V_1'$ and $r_2' V_2'$, respectively. The two viruses are killed by CTL responses at the rates $-p_1' V_1' X_1' - q' V_1' Y'$ and $-p_2' V_2' X_2' - q' V_2' Y'$, respectively. The CTLs are stimulated by their specific epitopes, and proliferate at the following rates: $c_1' X_1' V_1'$, $c_2' X_2' V_2'$, and $k' Y' (V_1' + V_2')$, respectively. The coefficients $c_1'$, $c_2'$, and $k'$ describe the immunogenicity rates of the epitopes. In the absence of antigenic stimuli, the activated CTLs die at the rates $-b' X_1'$, $-b' X_2'$, and $-b' Y'$, respectively. We introduce the term $\frac{1}{2}\varepsilon r_1' V_1' (1 + \xi'(t'))$ to describe the stochastic, frequent mutation from epitope variant $A_1$ to variant $A_2$. Here, $\xi'(t') = \sin(\Omega' t' + \sigma' W(t') + \Delta)$ is a bounded noise, where $\Omega'$ is the center frequency determined by the cell cycle, $\sigma'$ represents the intensity of frequency stochastic perturbation, $W(t')$ is the standard Wiener process with mean 0 and variance $t$ at time $t$, $\Delta$ is a random phase uniformly distributed in $[0, 2\pi]$, and the strength factor $\varepsilon \in [0, 1]$ represents the maximum mutation rate. All parameters are positive real numbers. A detailed explanation of stochastic mutation term is given in appendix A.

In order to facilitate dynamical analysis, we first non-dimensionalize Equation (1). Denote by $L$ a characteristic length constant and by $T$ a characteristic time constant. We introduce the following non-dimensional variables: $V_1 = \frac{c_1'}{r_1'} V_1'$, $V_2 = \frac{c_1'}{r_1'} V_2'$, $X_1 = \frac{p_1'}{r_1'} X_1'$, $X_2 = \frac{p_1'}{r_1'} X_2'$, $Y = \frac{p_1'}{r_1'} Y'$, and $t = r_1' t'$. Substituting these non-dimensional variables into Equation (1) yields

$$\begin{aligned}
\dot{V}_1 &= V_1 \left(1 - X_1 - qY\right) - \frac{1}{2}\varepsilon V_1 \left(1 + \xi(t)\right) \\
\dot{V}_2 &= V_2 \left(r - pX_2 - qY\right) + \frac{1}{2}\varepsilon V_1 \left(1 + \xi(t)\right) \\
\dot{X}_1 &= X_1 \left(V_1 - b\right) \\
\dot{X}_2 &= X_2 \left(cV_2 - b\right) \\
\dot{Y} &= Y \left[k \left(V_1 + V_2\right) - b\right]
\end{aligned} \tag{2}$$

where $\xi(t) = \sin(\Omega t + \sigma W(t) + \Delta)$. The non-dimensional parameters are defined as follows: $r = r_2'/r_1'$, $p = p_2'/p_1'$, $q = q'/p_1'$, $c = c_2'/c_1'$, $k = k'/c_1'$, $b = b'/r_1'$, $\Omega = \Omega'/r_1'$, and $\sigma = \sigma'/\sqrt{r_1'}$. The bounded noise $\xi(t)$ is a stationary process [28, 29]. The spectral density of $\xi(t)$ is

$$S(\omega) = \frac{\sigma^2}{4\pi} \frac{\omega^2 + \Omega^2 + \sigma^4/4}{[(\omega^2 - \Omega^2 - \sigma^4/4)^2 + \sigma^4\omega^2]} \tag{3}$$

The auto correlation function of $\xi(t)$ is

$$R(\tau) = \frac{1}{2} \exp\left(-\frac{\sigma^2}{2}|\tau|\right) \cos\Omega\tau \tag{4}$$

The bandwidth of $\xi(t)$ depends mainly on $\sigma$, the so-called bandwidth factor. We say $\xi(t)$ is a narrow band process when $\sigma$ is small, a wide band process when $\sigma$ large.

The non-dimensional deterministic system without bounded noise term is

$$\begin{aligned}
\dot{v}_1 &= v_1\left(1 - \frac{\varepsilon}{2} - x_1 - qy\right) \\
\dot{v}_2 &= v_2(r - px_2 - qy) + \frac{\varepsilon}{2}v_1 \\
\dot{x}_1 &= x_1(v_1 - b) \\
\dot{x}_2 &= x_2(cv_2 - b) \\
\dot{y} &= y[k(v_1 + v_2) - b]
\end{aligned} \tag{5}$$

System (5) has 5 saturated fixed points, which are stable against invasion by those variables that are close to zero; see Table 1. The saturated regions of these fixed points are mutually exclusive and cover the whole parameter space; see Fig. 1. Here, $P_i$ stands for the region, in which the fixed point $FP_i$ is saturated.

TABLE 1. The values of five saturated equilibriums of system (5).

| Fixed point | $v_1$ | $v_2$ | $x_1$ | $x_2$ | $y$ |
|---|---|---|---|---|---|
| $FP_1$ | $0$ | $\frac{b}{k}$ | $0$ | $0$ | $\frac{r}{q}$ |
| $FP_2$ | $\frac{b}{k} - \frac{b}{c}$ | $\frac{b}{c}$ | $0$ | $\frac{r-1}{p} + \frac{\varepsilon c}{2pk}$ | $\frac{2-\varepsilon}{2q}$ |
| $FP_3$ | $\frac{b}{k} + \frac{\varepsilon b}{2k(r-1)}$ | $\frac{\varepsilon b}{2k(1-r)}$ | $0$ | $0$ | $\frac{2-\varepsilon}{2q}$ |
| $FP_4$ | $b$ | $\frac{b}{k} - b$ | $1 - r + \frac{\varepsilon}{2(k-1)}$ | $0$ | $\frac{r}{q} - \frac{\varepsilon k}{2q(k-1)}$ |
| $FP_5$ | $b$ | $\frac{b}{c}$ | $\frac{2-\varepsilon}{2}$ | $\frac{r}{p} + \frac{\varepsilon c}{2p}$ | $0$ |

It can be seen from Table 1 and Fig. 1 that epitope $A$ is immunodominant in $P_5$ region whereas epitope $B$ dominates in $P_1$ and $P_3$ regions. In regions $P_2$ and $P_4$, the two epitopes $A$ and $B$ are codominant. Different parameter regions may correspond to responses in different patients.

3. **Dynamics of stochastic immune system.** In the absence of the stochastic mutation term, dynamics of system (5) exhibit either regular oscillations or fixed points. However, the stochastic mutation term will draw a different picture and lead to more complicated behaviors. We will use Monte Carlo simulations to show the new phenomena and to promote an intuitional understanding. In order to show the dynamical behaviors following the emergence of new virus mutant $v_2$, we assume

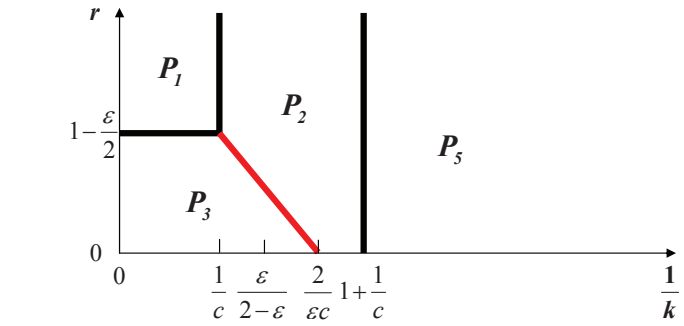


(a) $c > 2/\varepsilon - 1$

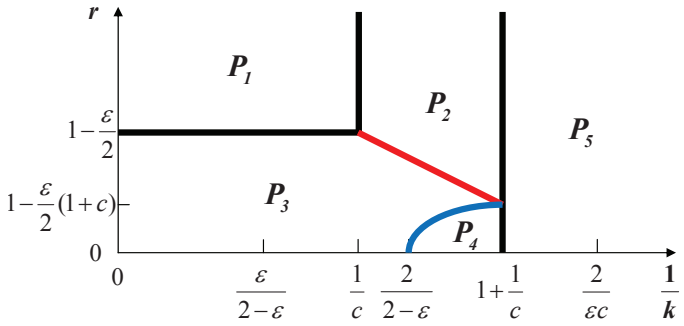


(b) $c < 2/\varepsilon - 1$

FIGURE 1. The parameter regions of the saturated fixed points of system (5) in which they possess existence and saturation. Note that there is a Hopf bifurcation at the critical control parameter value $c = 2/\varepsilon - 1$, and the saturated region of fixed point $FP_4$ only exhibits in the parameter space where $c < 2/\varepsilon - 1$. The red line corresponds to $r = -\frac{\varepsilon c}{2}\frac{1}{k} + 1$, and the blue curve is $r = 1 - \frac{\varepsilon}{2-2k}$. (a) if $c > 2/\varepsilon - 1$; (b) if $c < 2/\varepsilon - 1$.

that all possible CTLs are present in the beginning ($t = 0$), and there exists only one variant $A_1$ of epitope $A$. Thus, at this initial stage, the system is reduced to

$$\begin{aligned} \dot{v}_1 &= v_1 (1 - x_1 - qy) \\ \dot{x}_1 &= x_1 (v_1 - b) \\ \dot{x}_2 &= -bx_2 \\ \dot{y} &= y (kv_1 - b) \end{aligned} \tag{6}$$

The pre-existing CTL $x_2$ will decline exponentially in the absence of the virus mutant $v_2$. There are two neutrally stable saturated equilibriums

$$\begin{aligned} (v_1, x_1, x_2, y) &= (b, 1, 0, 0), \qquad if \quad k < 1 \\ (v_1, x_1, x_2, y) &= (b/k, 0, 0, 1/q), \quad if \quad k > 1 \end{aligned} \tag{7}$$

Epitope $A$ is immunodominant when $k < 1$; otherwise, epitope $B$ is immunodominant.

In the following, we investigate the effects of stochastic mutations using Monte Carlo simulations. We assume that, at the initial infection, the amount of viruses

and CTLs are $v_1 = 0.001$, $v_2 = 0$, $x_1 = 0.001$, $x_2 = 0.001$, and $y = 0.001$. Then, after 200 time units, a stochastic mutation term is introduced to the system so that the dynamics is governed by Eq. (2) since then.

3.1. $P_1$ **region.** Since the fixed point $FP_1$ of system (5) is neutrally stable, the responses exhibit neutral oscillations around their long-term averages, where CTLs $X_1$ and $X_2$ are vanished. There is clearly a complete shift of immunodominance from epitope $A$ to epitope $B$ while $k < 1$. Figure 2(a) shows that the shift happens just as the mutation takes place at $(t = 200)$. Despite stochastic noises, the oscillations exhibit regular patterns. Moreover, the mutation also eliminates the original virus variant $V_1$, and the emergent mutant $V_2$ oscillates with a larger amplitude.

3.2. $P_2$ **region.** The fixed point $FP_2$ is an asymptotically stable fixed point of system (5). Since the CTLs $X_2$ and $Y$ have positive values in the steady state, there is a partial shift of immunodominance regardless of $k$ (partial shift means that the old response against epitope A, with specificity for the original variant, coexists with a response against epitope B [1]). The immunodominance is partially shifted from epitope $A$ to epitope $B$ while $k < 1$, together with a new specific CTL response against epitope $A$ (old response against variant $A_1$ is replaced by new response against variant $A_2$), and partially shifted from epitope $B$ to epitope $A$ when $k > 1$. We also notice an interesting "immunodominance interchange" phenomenon, as seen in Fig. 3(a). The complete shift of immunodominance from epitope $A$ to epitope $B$ takes place soon after the mutation happens at $t = 200$. However, the converse process takes place almost 400 time units later, and epitope B captures the immunodominance at approximately $t = 600$. Epitope B loses its immunodominance after 200 time units and finally the system converges to the fixed point $FP_2$. The virus concentrations exhibit similar pattern. Virus $V_1$ experiences quite a long time of "latency", before it suddenly shows up approximately at $t = 800$. The asymptotic property of the fixed point $FP_2$ ensures that the system converges to a statistically steady state. The probability density of the concentrations are depicted in Figs. 4. The stationary probability density of virus with $\sigma = 0.1$ is bimodal, which implies that the virus has two more probable concentration levels. It is interesting to note that the variance of oscillation is not monotonically increasing with a concomitant increase in $\sigma$, which suggests increasing strength of stochastic perturbation. The maximum variance is achieved with a specific strength of $\sigma$. The phenomenon suggests that the magnitude of virus fluctuations may be greatly influenced by the bandwidth of the noise, which is due to $\sigma$-dependent spectral density and will be further explained in Sec. 3.3.

3.3. $P_3$ **region.** In this region, the mutant stimulates the response against epitope $B$. When $k < 1$, the response in $B$ displaces the original response in $A$, representing a complete shift in immunodominance from epitope $A$ to epitope $B$. While the neutrally stable fixed point $FP_3$ introduces regular periodic oscillations to system (5), the stochastic mutation in system (2) disrupts its regularity and makes the viruses perform nearly unrestricted growth. It is clear to see from Fig. 5(b) that the total virus amount first shrinks immediately after the mutation, and then booms over tens of times than before. Clinically, this represents an undetectable latency period, which is followed by a rapid growing period with the concomitant constitutional symptoms.

We assume that there is a threshold of the concentration of virus, beyond which the host is critically ill. The probability that the virus levels reach the threshold is

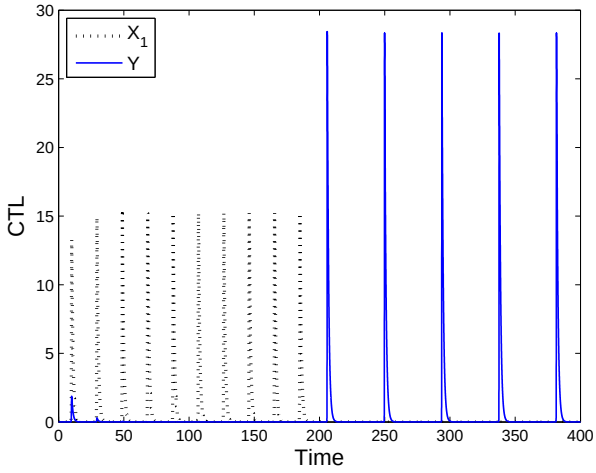


(a) Evolution of CTL concentration

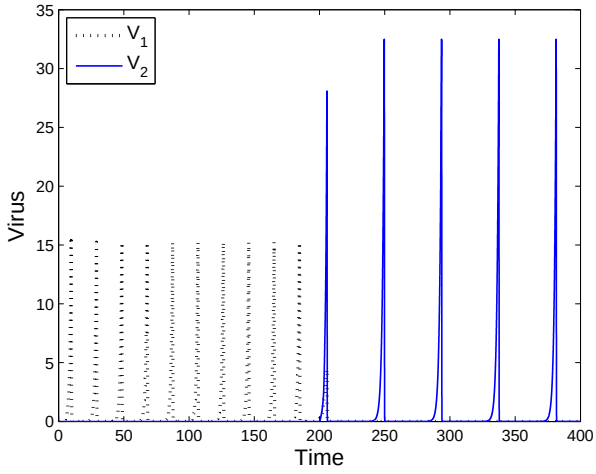


(b) Evolution of viral concentration

FIGURE 2. Immune responses in the $P_1$ region, parameter settings: $c = 0.8$, $r = 0.75$, $k = 0.9$, $p = 1$, $q = 1$, $b = 1$, $\varepsilon = 1$, $\Omega = \pi$, $\sigma = 1$. (a) Complete shift in immunodominance from epitope $A$ to epitope $B$. The CTL responses exhibit regular oscillations around the neutrally stable fixed point $FP_1$. (b) Virus $V_1$ vanishes, while virus $V_2$ emerges and oscillates with larger amplitude.

a function of time. The stochastic mutation will increase the probability of critical illness. It is reasonable to assume that the host will rapidly become critically ill when the peak of the spectral density of the bounded noise $\xi(t)$ overlaps the eigen-frequency of system (5). The center frequency $\Omega$ and the bandwidth factor $\sigma$ will determine the spectral density according to Eq. (3). We keep $\Omega = \pi$ and study the

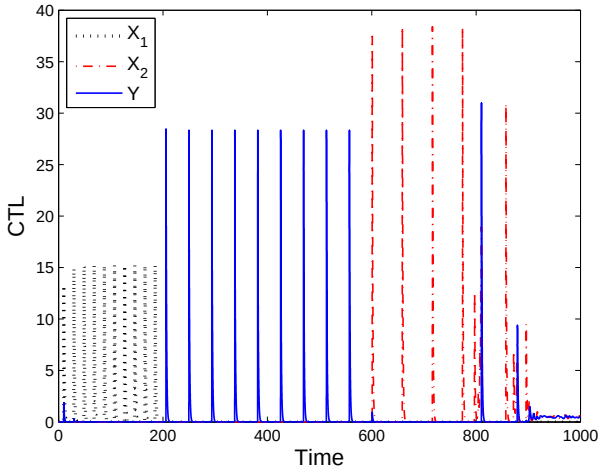


(a) Evolution of CTL concentration

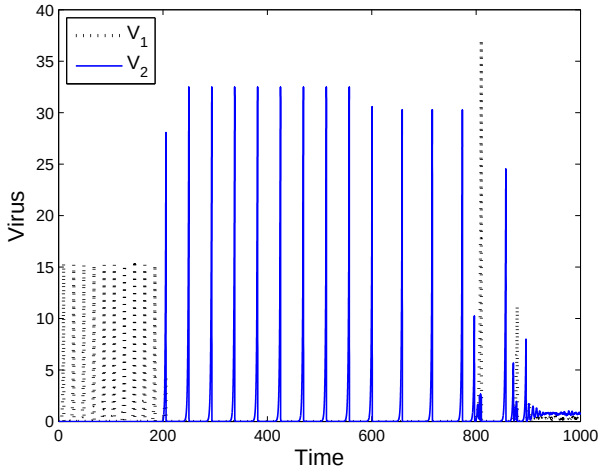


(b) Evolution of viral concentration

FIGURE 3. Immune responses in the $P_2$ region, parameter settings: $c = 1.3$, $r = 0.75$, $k = 0.9$, $p = 1$, $q = 1$, $b = 1$, $\varepsilon = 1$, $\Omega = \pi$, $\sigma = 1$. (a) "Immunodominance interchange" between epitopes $A$ and $B$. The immune responses converge to asymptotic stable equilibrium $FP_2$: $X_1 = 0$, $X_2 = 0.47$, and $Y = 0.5$. (b) Virus $V_1$ experiences a period of "latency", before showing up again and converging to fixed point $FP_2$: $V_1 = 0.34$, $V_2 = 0.77$.

influence of the bandwidth factor $\sigma$. The period of system (5) can be simply estimated from the inset in Fig. 6(a) $T_0 \approx 47.5$, and the relationship of $\sigma$ to the spectral density of bounded noise $\xi(t)$ can be plotted by setting $\Omega = \pi$ and $\omega = 2\pi/47.5$ in Eq. (3). The peak value is $\sigma \approx 2.5$. The host will more likely to evolve into

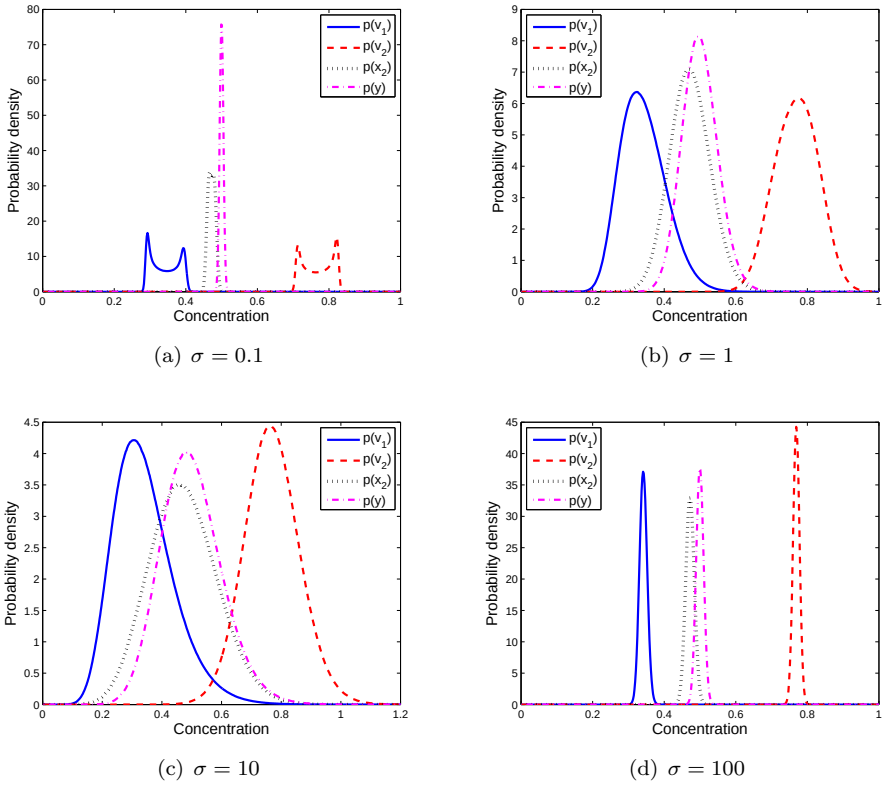


(a) $\sigma = 0.1$ (b) $\sigma = 1$

(c) $\sigma = 10$ (d) $\sigma = 100$

FIGURE 4. Probability densities of stationary distributions of concentrations in the $P_2$ region, parameter settings: $c = 1.3$, $r = 0.75$, $k = 0.9$, $p = 1$, $q = 1$, $b = 1$, $\varepsilon = 1$, $\Omega = \pi$. (a) The bounded noise in the stochastic mutation term is a narrow band one for $\sigma = 0.1$. (b) Noise for $\sigma = 1$. (c) Noise for $\sigma = 10$. (d) Wide band noise for $\sigma = 100$.

critical illness in this situation. The conclusion can be validated by Fig. 6(b). The $\sigma$-dependent spectral density may also explain the phenomenon observed in Fig. 4. Since the parametric resonance of nonlinear system under parametric excitation of narrow band bounded noise will occur, the maximum critical illness probability will be achieved with specific value of $\Omega$ [30].

3.4. $P_4$ **region.** In the $P_4$ region, the partial shift of immunodominance from epitope $A$ to epitope $B$ always occurs. The original response against epitope $A$ coexists with a response against epitope $B$. We observe the "immunodominance interchange" phenomenon again. As depicted in Fig. 7(a), the epitope B becomes immunodominant at the first stage after mutation. The CTL response directed against epitope $A$ emerges after a long period of "latency", and is codominant with the one against epitope $B$. However, the epitope $B$ dominates again since $t \approx 6000$. The stochastic perturbation disturbs the stable limit cycle which surrounds the unstable fixed point $FP_4$, and the virus booms over 50 times together with the "immunodominance interchange" process.

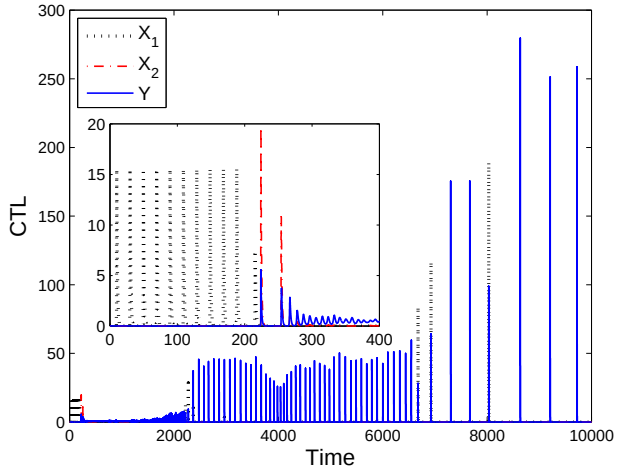


(a) Evolution of CTL concentration

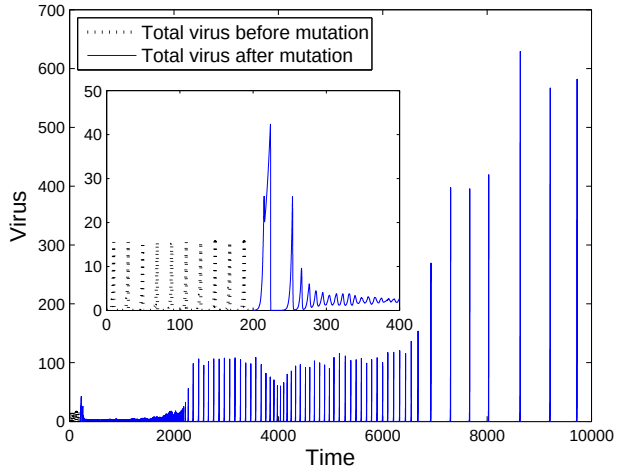


(b) Evolution of viral concentration

FIGURE 5. Immune responses in the $P_3$ region, parameter settings: $c = 0.8$, $r = 0.095$, $k = 0.45$, $p = 1$, $q = 1$, $b = 1$, $\varepsilon = 1$, $\Omega = \pi$, $\sigma = 1$. (a) Complete shift of immunodominance from epitope $A$ to epitope $B$. The immune responses oscillate irregularly and the peak value increases tens of times ever since mutation. (b) The change of total virus amount, $V_1+V_2$, due to mutation. The amount increases over 40 times in concentration.

3.5. $P_5$ **region.** The fixed point $FP_5$ is neutrally stable for system (5). A sample orbit is depicted in Fig. 8(a). There is no shift of immunodominance in $P_5$ region. What differs from other regions is a "pulse" fluctuation in the evolution of virus mutant, as illustrated in Fig. 8(b). The virus mutant $V_2$ takes a surprising jump,

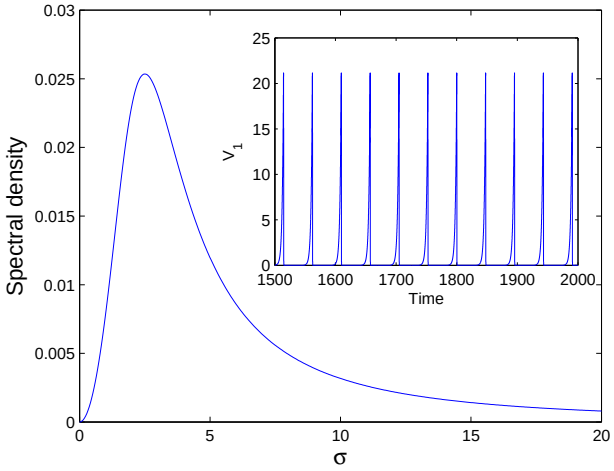


(a) Spectral density of bounded noise $\xi(t)$ at $\omega = 2\pi/47.5$

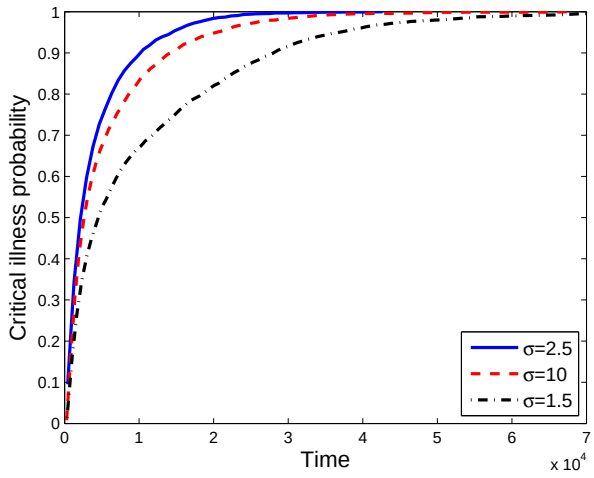


(b) Critical illness probability

FIGURE 6. Critically ill probability in the $P_3$ region, parameter settings: $c = 0.8$, $r = 0.095$, $k = 0.45$, $p = 1$, $q = 1$, $b = 1$, $\varepsilon = 1$, $\Omega = \pi$. (a) The relationship of bandwidth factor $\sigma$ to the spectral density of bounded noise $\xi(t)$ at $\omega = 2\pi/47.5$, the eigenfrequency of system (5). The inset shows the stationary behavior of system (5), from which the period can be estimated as $T_0 \approx 47.5$. (b) The critical illness probability for $\sigma = 2.5$, 10 and 1.5, respectively. The threshold of the concentration of virus is $V_1 + V_2 = 100$.

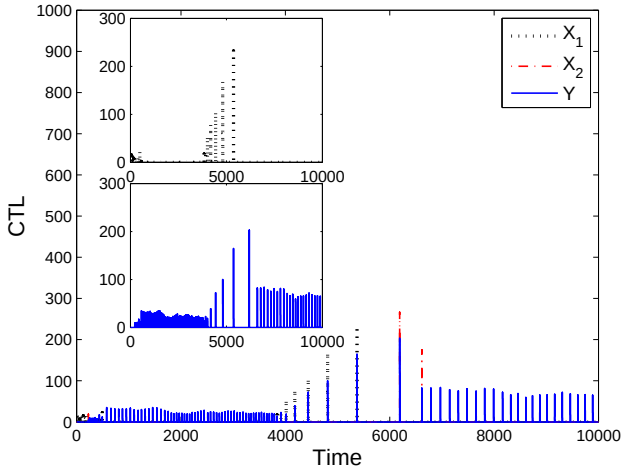


(a) Evolution of CTL concentration

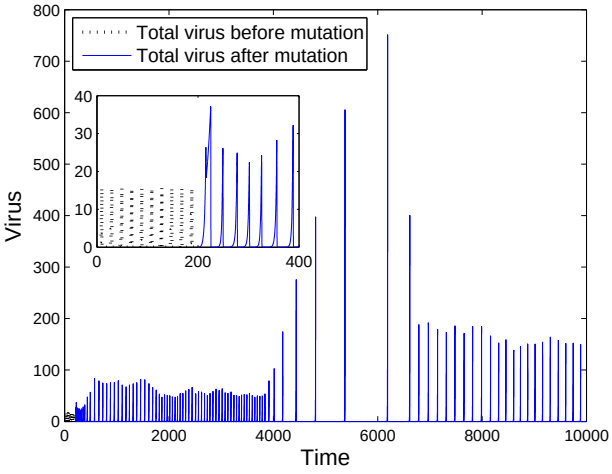


(b) Evolution of viral concentration

FIGURE 7. Immune responses in the $P_4$ region, parameter settings: $c = 0.8$, $r = 0.08$, $k = 0.45$, $p = 1$, $q = 1$, $b = 1$, $\varepsilon = 1$, $\Omega = \pi$, $\sigma = 1$. (a) Partial shift of immunodominance from epitope $A$ to epitope $B$. At the first stage after mutation (from $t = 200$ to 4000), the epitope B takes immunodominance. However, the CTL directed to epitope $A$ recurs and is codominant with the one directed to epitope $B$, and takes over the immunodominance, but the epitope $B$ dominates again since $t \approx 6000$. (b) The change of total virus amount, $V_1 + V_2$, due to mutation. The amount increases up to 50 times in concentration together with a concomitant "Immunodominance interchange" process.

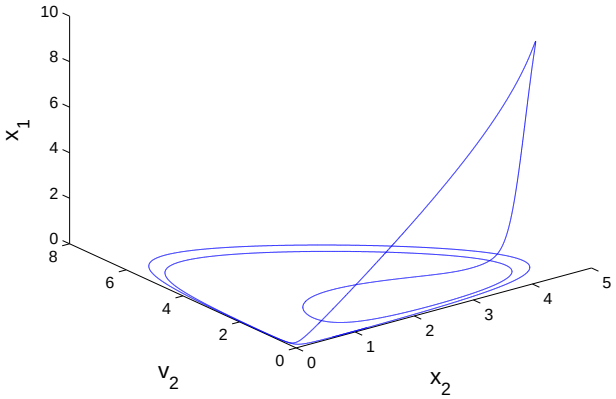


(a) A sample orbit in the $P_5$ region

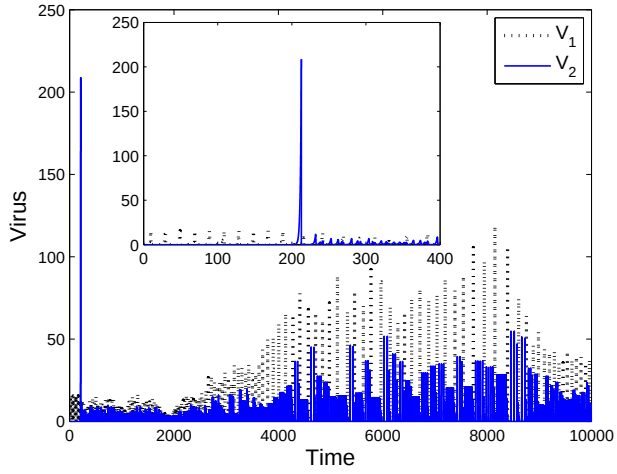


(b) Evolution of viral concentration

FIGURE 8. Immune responses in the $P_5$ region, parameter settings: $c = 0.8$, $r = 0.75$, $k = 0.4$, $p = 1$, $q = 1$, $b = 1$, $\varepsilon = 1$, $\Omega = \pi$, $\sigma = 1$. (a) A sample trajectory in the region of $P_5$ of system (5). (b) The "pulse" fluctuation of virus mutant $V_2$.

which is over 10 times larger than the original $V_1$ variant in concentration. The phenomenon indicates that a rapid increasing of the escape mutant may be detected soon after mutation; however, the high concentration may not last long.

3.6. **Stochastic migration of state.** Since the intrinsic effect of the stochastic term is perturbation in the intensity of mutation $\varepsilon$, a direct consequence of stochastic mutation is the migration between parameter regions. The long-term behavior

TABLE 2. Conditions of immunodominance shift due to stochastic mutation.

| Parameter region | $k < 1$ | $k > 1$ |
|---|---|---|
| $P_1$ | $A_1 \xrightarrow{Complete\ shift} B$ | |
| $P_2$ | $A_1 \xrightarrow{Partial\ shift} \langle A_2, B\rangle$ | $B \xrightarrow{Partial\ shift} \langle A_2, B\rangle$ |
| $P_3$ | $A_1 \xrightarrow{Complete\ shift} B$ | |
| $P_4$ | $A_1 \xrightarrow{Partial\ shift} \langle A_1, B\rangle$ | |
| $P_5$ | $A_1 \Longrightarrow \langle A_1, A_2\rangle$ | |

will jump back and forth between adjacent regions randomly, which makes the system response very irregular and unpredictable. The phenomenon is probably more significant when the parameters of system are located in the vicinity of the boundaries of the regions. However, $P_5$ region is relatively stable since it is independent of $\varepsilon$. Since each patient corresponds to a specific parameter setting, the stochastic migration between parameter regions will show the stochastic variability of immune system with the evolution of infection.

4. **Conclusions.** We introduce a bounded noise term to the immunodominance model developed by Nowak et al., to account for the intrinsic stochastic mutations of the immune system. The current study is different from previous research in that we consider continuous occurrence of mutation instead of sporadic events [1, 22].

We study the effects of a stochastic mutation term on immunodominance, as summarized in Table 2. There are five mutually exclusive parameter regions of the corresponding deterministic system, and each region has a saturated boundary fixed point. The variable epitope $A$ may shift immunodominance to conserved epitope $B$. In parameter regions of $P_1$ and $P_3$, there are complete shift in immunodominance from epitope $A$ to epitope $B$ if $k < 1$. In parameter region of $P_2$, there is partial shift of immunodominance from epitope $A$ to epitope $B$ if $k < 1$, and the contrary is the case if $k > 1$. In parameter region of $P_4$, there is always partial shift of immunodominance from epitope $A$ to epitope $B$. In the region of $P_5$, there is no shift in immunodominance occur, but a diversification in immune responses against epitope $A$. In parameter regions of $P_2$ and $P_4$, the interesting "immunodominance interchange" phenomenon is observed.

Since the spectral density of bounded noise $\xi(t)$ is dependent on the center frequency $\Omega$ and the bandwidth factor $\sigma$, the immune response is also influenced by these parameters. Specified value of $\Omega$ and $\sigma$ will apparently increase the concentration of virus and probably make the host enter into critically ill condition.

We also study the dynamics of stochastic mutation system. The system has complicated behaviors and exhibit interesting features, such as the "pulse" fluctuation phenomenon. The evolutions of CTLs and viruses may experience "latency" or "booming" period, and the state will migrate between adjacent parameter regions stochastically, which makes the evolution of the immune system unpredictable. However, the regular patterns analyzed in this work may promote our understanding of the long-term trend of the immune system. The systems within parameter regions $P_3$, $P_4$, and $P_5$ may experience unbounded increases in the viral concentrations. However, the systems in the regions of $P_1$ and $P_2$ may have their viral concentrations controlled in a limit range. The distinct long-term evolutionary

trends of different parameter regions suggest that a possible immunotherapy to treat the patients and to improve their conditions to satisfy the requirements of parameter region $P_2$. Numerical studies on stochastic mutations may lead to better understanding of immunodominance and may help to advance the development of immunotherapy.

**Acknowledgments.** This work was in part supported by NSF under grant number CMMI-0845753.

**Appendix** A. **Stochastic mutation term.** There are three critical parameters: the strength factor $\varepsilon$, the bandwidth factor $\sigma$, and the center frequency $\Omega$. The strength factor $\varepsilon \in [0, 1]$ is the maximum mutation rate. The stochastic mutation term describes a stochastic fluctuation around the average mutation rate $\varepsilon/2$, which should be estimated according to the experimental data.

The mathematical expectation of bounded noise at a fixed time $t$ is:

$$\begin{aligned} E[\xi(t)] &= \int_{-\infty}^{\infty} \sin(\Omega t + \sigma x + \Delta) \frac{1}{\sqrt{2\pi t}} e^{-x^2/2t} dx \\ &= e^{-t\sigma^2/2} \sin(\Omega t + \Delta) \\ &= \begin{cases} 0 & \sigma \to \infty \\ \sin(\Omega t + \Delta) & \sigma \to 0 \end{cases} \end{aligned} \tag{8}$$

And the auto correlation function (4)

$$R(\tau) = \frac{1}{2} \exp\left(-\frac{\sigma^2}{2} |\tau|\right) \cos \Omega\tau = \begin{cases} \dfrac{1}{2}\delta_{\tau,0} & \sigma \to \infty \\ \dfrac{1}{2} \cos \Omega\tau & \sigma \to 0 \end{cases} \tag{9}$$

where $\delta_{\tau,0}$ is Kronecker delta. Thus, the bounded noise $\xi(t)$ tends to a finite power white noise as $\sigma \to \infty$, and becomes a harmonic noise as $\sigma \to 0$.

It can be concluded from spectral density expression, Eq. (3), that the bandwidth of process $\xi(t)$ depends mainly on $\sigma$, so we also call $\sigma$ bandwidth factor. It is a narrow band process when $\sigma$ is small and a wide band process when $\sigma$ is large.

The flexible and adjustable characteristics of bounded noise make it an appropriate description of the intrinsically random mutation rate and a good approximation to cell cycles according to heterogeneous scenarios.

Cell cycle is obviously periodic; however, the endogenous and exogenous signal that influences the mutation may be aperiodic. Thus, it is reasonable to assume that the mutation rate is a stochastic perturbation to periodic fluctuations. In case the mutation rate observed in experiments shows regular periodic fluctuations around a mean value, a small $\sigma$ should be adopted. Then, the center frequency $\Omega$ is determined by the cell cycle $T_{\text{cell cycle}}$

$$\Omega = \frac{2\pi}{T_{\text{cell cycle}}} = \frac{2\pi(\text{proliferation rate} - \text{death rate})}{\ln 2} \tag{10}$$

Alternatively, when there do not exist regular fluctuations or a characteristic frequency band, a large $\sigma$ will be chosen to capture the stochastic nature.

**Appendix** B. **Parameters and Monte Carlo simulation.** Parameters and variables are non-dimensionalized to facilitate dynamic analyses. The parameters $c_1'$, $r_1'$, and $p_1'$ are selected as the characteristic parameters. Other parameters are scaled relative to these characteristic parameters. Note that the units of the characteristic parameters are $c_1'$ $(L^3T^{-1})$, $r_1'$ $(T^{-1})$, and $p_1'$ $(L^3T^{-1})$. Then, one can obtain the concentrations of all the variables in SI units as $V_1' = \frac{r_1'}{c_1'}V_1$, $V_2' = \frac{r_1'}{c_1'}V_2$, $X_1' = \frac{r_1'}{p_1'}X_1$, $X_2' = \frac{r_1'}{p_1'}X_2$, $Y' = \frac{r_1'}{p_1'}Y$.

Since the Wiener process is the formal derivative of Gaussian white noise

$$\frac{dW(t)}{dt} = \zeta(t) \tag{11}$$

where $W(t)$ is the standard Wiener process, and $\zeta(t)$ is the standard Gaussian white noise. System (2) can be extended as

$$\begin{aligned}
\dot{V}_1 &= V_1(1 - X_1 - qY) - \frac{1}{2}\varepsilon V_1(1 + \sin Z)\\
\dot{V}_2 &= V_2(r - pX_2 - qY) + \frac{1}{2}\varepsilon V_1(1 + \sin Z)\\
\dot{X}_1 &= X_1(V_1 - b)\\
\dot{X}_2 &= X_2(cV_2 - b)\\
\dot{Y} &= Y[k(V_1 + V_2) - b]\\
\dot{Z} &= \Omega + \sigma\zeta(t)
\end{aligned} \tag{12}$$

To demonstrate the dynamic behaviors, we choose representative parameter combinations from corresponding parameter regions. The stochastic dynamics are studied using Monte Carlo simulations. The corresponding time series of the population density are obtained by integrating Eqs. (12) numerically using the fourth order Runge-Kutta scheme. The stationary probabilities are estimated with sample averages over 120 realizations, with integration time step 0.005 and integration time up to 30000 for each realization.

## REFERENCES


[1] M. A. Nowak, R. M. May and K. Sigmund, *Immune responses against multiple epitopes*, J. Theor. Biol., **175** (1995), 325–353.

[2] M. A. Nowak, *Immune responses against multiple epitopes: a theory for immunodominance and antigenic variation*, Semin. Virol., **7** (1996), 83–92.

[3] D. Wodarz, "Killer Cell Dynamics: Mathematical and Computational Approaches to Immunology," Springer, New York, USA, 2007.

[4] L. Adorini, E. Appella, G. Doria and Z. A. Nagy, *Mechanisms influencing the immunodominance of T cell determinants*, J. Exp. Med., **168** (1988), 2091–2104.

[5] A. J. McMichael and R. E. Phillips, *Escape of human immunodeficiency virus from immune control*, Annu. Rev. Immunol., **15** (1997), 271–296.

[6] P. J. R. Goulder, et al., *Late escape from an immunodominant cytotoxic T-lymphocyte response associated with progression to AIDS*, Nature Med., **3** (1997), 212–217.

[7] P. J. R. Goulder, et al., *Patterns of immunodominance in HIV-1-specific cytotoxic T lymphocyte responses in two human histocompatibility leukocyte antigens (HLA)-identical siblings with HLA-A*0201 are influenced by epitope mutation*, J. Exp. Med., **185** (1997), 1423–1433.

[8] J. W. Yewdell and J. R. Bennink, *Immunodominance in major histocompatibility complex class I-restricted T lymphocyte responses*, Annu. Rev. Immunol., **17** (1999), 51–88.

[9] S. Gupta and R. M. Anderson, *Population structure of pathogens: the role of immune selection*, Parasitology Today, **15** (1999), 497–501.

[10] C. C. Bergmann, J. D. Altman, D. Hinton and S. A. Stohlman, *Inverted immunodominance and impaired cytolytic function of CD8+ T cells during viral persistence in the central nervous system*, J. Immunol. **163** (1999), 3379–3387.
[11] W. S. Chen, L. C. Antón, J. R. Bennink and J. W. Yewdell, *Dissecting the multifactorial causes of immunodominance in class I-restricted T cell responses to viruses*, Immunity, **12** (2000), 83–93.
[12] X. G. Yu, et al., *Consistent patterns in the development and immunodominance of human immunodificiency virus type 1 (HIV-1)-specific CD8+ T-cell responses following acute HIV-1 infection*, J. Virol., **76** (2002), 8690–8701.
[13] M. A. Brehm, A. K. Pinto, K. A. Daniels, J. P. Schneck, R. M. Welsh and L. K. Selin, *T cell immunodominance and maintenance of memory regulated by unexpectedly cross-reactive pathogens*, Nature Immunol., **3** (2002), 627–634.
[14] U. Karrer, et al., *Memory inflation: continuous accumulation of antiviral CD8+ T cells over time*, J. Immunol., **170** (2003), 2022–2029.
[15] E. J. Wherry, J. N. Blattman, K. Murali-Krishna, R. van der Most and R. Ahmed, *Viral persistence alters CD8 T-cell immunodominance and tissue distribution and results in distinct stages of functional impairment*, J. Virol., **77** (2003), 4911–4927.
[16] P. K. C. Goon, et al., *Human T cell lymphotropic virus (HTLV) type-1-specific CD8+ T cells: frequency and immunodominance hierarchy*, J. Infect. Dis., **189** (2004), 2294–2298.
[17] R. Draenert, et al., *Constraints on HIV-1 evolution and immunodominance revealed in monozygotic adult twins infected with the same virus*, J. Exp. Med., **203** (2006), 529–539.
[18] M. A. Nowak, R. M. Anderson, A. R. McLean, T. F. W. Wolfs, J. Goudsmit and R. M. May, *Antigenic diversity thresholds and the development of AIDS*, Science, **254** (1991), 963–969.
[19] M. A. Nowak, et al., *Antigenic oscillations and shifting immunodominance in HIV-1 infections*, Nature, **375** (1995), 606–611.
[20] D. Wodarz and M. A. Nowak, *CD8 memory, immunodominance, and antigenic escape*, Eur. J. Immunol., **30** (2000), 2704–2712.
[21] M. A. Nowak and R. M. May, "Virus Dynamics: Mathematical Principles of Immunology and Virology," Oxford University Press, New York, USA, 2000.
[22] C. L. Althaus and R. J. De Boer, *Dynamics of immune escape during HIV/SIV infection*, PLOS Comput. Biol., **4** (2008), e1000103.
[23] A. Handel and R. Antia, *A simple methematical model helps to explain the immunodominance of CD8 T cells in influenza a virus infections*, J. Virol., **82** (2008), 7768–7772.
[24] M. A. Nowak, R. M. May and R. M. Anderson, *The evolutionary dynamics of HIV-1 quasispecies and the development of immunodeficiency disease*, AIDS, **4** (1990), 1095–1103.
[25] M. A. Nowak and R. M. May, *Coexistence and competition in HIV infections*, J. Theor. Biol., **159** (1992), 329–342.
[26] M. A. Nowak and R. M. May, *AIDS pathogenesis: mathematical models of HIV and SIV infections*, AIDS 7, Suppl., **1** (1993), S3–S18.
[27] R. M. Anderson, *Mathematical studies of parasitic infection and immunity*, Science, **264** (1994), 1884–1886.
[28] Y. K. Lin and G. Q. Cai, "Probabilistic Structural Dynamics: Advanced Theory and Applications," McGraw-Hill, New York, 1995.
[29] W. Q. Zhu, Z. L. Huang, J. M. Ko and Y. Q. Ni, *Optimal feedback control of strongly non-linear systems excited by bounded noise*, J. Sound Vib., **274** (2004), 701–724.
[30] Z. L. Huang, W. Q. Zhu, Y. Q. Ni and J. M. Ko, *Stochastic averaging of strongly non-linear oscillators under bounded noise excitation*, J. Sound Vib., **254** (2002), 245–267.

Received September 21, 2009; Accepted September 11, 2010.

*E-mail address*: walton731@hotmail.com
*E-mail address*: communicating author: xzhao9@utk.edu
*E-mail address*: mjzhang@utk.edu